

## **A First-Order Assessment of Direct Aerosol Radiative Effect in the Southeastern U.S. Using over a Decade Long Multisatellite Data Record**

Authors: Alston, Erica J., and Sokolik, Irina N.

Source: Air, Soil and Water Research, 9(1)

Published By: SAGE Publishing

URL: <https://doi.org/10.1177/ASWR.S39226>

---

BioOne Complete ([complete.BioOne.org](https://complete.BioOne.org)) is a full-text database of 200 subscribed and open-access titles in the biological, ecological, and environmental sciences published by nonprofit societies, associations, museums, institutions, and presses.

Your use of this PDF, the BioOne Complete website, and all posted and associated content indicates your acceptance of BioOne's Terms of Use, available at [www.bioone.org/terms-of-use](https://www.bioone.org/terms-of-use).

Usage of BioOne Complete content is strictly limited to personal, educational, and non - commercial use. Commercial inquiries or rights and permissions requests should be directed to the individual publisher as copyright holder.

---

BioOne sees sustainable scholarly publishing as an inherently collaborative enterprise connecting authors, nonprofit publishers, academic institutions, research libraries, and research funders in the common goal of maximizing access to critical research.

# A First-Order Assessment of Direct Aerosol Radiative Effect in the Southeastern U.S. Using Over a Decade Long Multisatellite Data Record

Erica J. Alston<sup>1</sup> and Irina N. Sokolik<sup>2</sup>

<sup>1</sup>NASA Langley Research Center, Hampton, VA, USA. <sup>2</sup>Georgia Institute of Technology, School of Earth and Atmospheric Sciences, Atlanta, GA, USA.

**ABSTRACT:** Aerosols comprise a critical portion of the Earth's climate due to their radiative properties. More emphasis is now being placed upon understanding radiative effects of aerosols on a regional scale. The primary goal of this research is to estimate the aerosol direct radiative effect (DRE) and examine its dynamical nature in the Southeastern U.S. based on satellite data obtained from the moderate-resolution imaging spectroradiometer (MODIS) and multi-angle imaging spectroradiometer (MISR) instruments onboard the Terra satellite from 2000 to 2011. This 12-year analysis utilizes satellite measurements of aerosol optical depth (AOD), surface albedo, cloud fraction, and single-scattering albedo over the Southeastern U.S. as inputs to a first-order approximation of regional top of the atmosphere DRE. Results indicate that AOD is the primary driver of DRE estimates, with surface albedo and single-scattering albedo having some appreciable effects as well. During the cooler months, the minima (less negative) of DRE vary between  $-6$  and  $-3$   $\text{W/m}^2$ , and during the warmer months, there is more variation with DRE maxima varying between  $-24$  and  $-12.6$   $\text{W/m}^2$  for MODIS and  $-22.5$  and  $-11$   $\text{W/m}^2$  for MISR. Yet if we take an average of the monthly DRE over time (12 years), we estimate  $\Delta F = -7.57$   $\text{W/m}^2$  for MODIS and  $\Delta F = -5.72$   $\text{W/m}^2$  for MISR. Regional assessments of the DRE show that background levels of DRE are similar to the 12-year average of satellite-based DRE, with urbanized areas having increased levels of DRE compared to background conditions. Over the study period, DRE has a positive trend (becoming less negative), which implies that the region could lose this protective top of the atmosphere cooling with the advancement of climate change impacting the biogenic emissions of aerosols.

**KEYWORDS:** aerosols, aerosol direct radiative effect, MODIS, MISR, climate

**CITATION:** Alston and Sokolik. A First-Order Assessment of Direct Aerosol Radiative Effect in the Southeastern U.S. Using Over a Decade Long Multisatellite Data Record. *Air, Soil and Water Research* 2016;9:97–112 doi:10.4137/ASWR.S39226.

**TYPE:** Original Research

**RECEIVED:** June 16, 2016. **RESUBMITTED:** September 6, 2016. **ACCEPTED FOR PUBLICATION:** September 11, 2016.

**ACADEMIC EDITOR:** Carlos Alberto Martinez-Huitle, Editor in Chief

**PEER REVIEW:** Two peer reviewers contributed to the peer review report. Reviewers' reports totaled 541 words, excluding any confidential comments to the academic editor.

**FUNDING:** Support for Dr. Sokolik was provided by NASA LCLUCK. The authors confirm that the funder had no influence over the study design, content of the article, or selection of this journal.

**COMPETING INTERESTS:** Authors disclose no potential conflicts of interest.

**COPYRIGHT:** © the authors, publisher and licensee Libertas Academica Limited. This is an open-access article distributed under the terms of the Creative Commons CC-BY-NC 3.0 License.

**CORRESPONDENCE:** erica.j.alston@nasa.gov

Paper subject to independent expert single-blind peer review. All editorial decisions made by independent academic editor. Upon submission manuscript was subject to anti-plagiarism scanning. Prior to publication all authors have given signed confirmation of agreement to article publication and compliance with all applicable ethical and legal requirements, including the accuracy of author and contributor information, disclosure of competing interests and funding sources, compliance with ethical requirements relating to human and animal study participants, and compliance with any copyright requirements of third parties. This journal is a member of the Committee on Publication Ethics (COPE).

Provenance: the authors were invited to submit this paper.

Published by Libertas Academica. Learn more about this journal.

## Introduction

Aerosols play an important role in the radiative balance of the Earth. Aerosol's radiative effects are related to multiple factors, eg, the aerosol's chemical composition, altitude in the atmosphere, morphology, size, etc. While large global models attempt to accurately portray global aerosol climatic effects, effects of aerosol are just as important on smaller regional scales. At this spatial resolution, the nature of aerosols that impact daily air quality also plays a role in the region's longer term climate. Like the majority of the Eastern U.S., ground-based particulate matter monitors in the Southeastern (SE) U.S. are dominated by organic carbon and sulfate, with a small portion comprising black carbon.<sup>1</sup> Additional measures of aerosol concentration inferred through aerosol optical depth (AOD) provided via satellites have data records over 12 years. This satellite record provides a broader regional perspective of the longer term behavior of aerosols in the region, which lends it useful for understanding the radiative impacts of these regional aerosols.

Many radiation studies have typically focused on the radiative balance at the top of the atmosphere (TOA) on a

global basis. Recently, these studies are focusing more on the regional nature of aerosol radiative impacts. Carrico et al<sup>2</sup> estimated instantaneous TOA forcing based on daily point measurements of aerosol extinction with a sun photometer in Atlanta, GA, during the six-week 1999 Atlanta Supersite Experiment. These measurements are only representative of the immediate urban environment and do not sample the regional aerosols. Additionally, these are short-duration measurements; longer in time and larger spatial resolution data records are needed to draw broader conclusions about regional aerosol impacts. To better address this need, Goldstein et al<sup>3</sup> used a mean value of summer aerosols from seven years (2000–2007) of AOD measured by the multi-angle imaging spectroradiometer (MISR) and moderate-resolution imaging spectroradiometer (MODIS) instruments on the NASA Terra satellite to estimate the regionally averaged clear sky radiative effect of  $-3.9$   $\text{W/m}^2$ . They interpreted this change in forcing as the effect of secondary organic aerosols (SOA) formed from biogenic emission during the summertime in the SE U.S. Their calculated radiative effect is less than the estimate from



the study by Carrico et al<sup>2</sup> ( $\Delta F = -11 \pm 6 \text{ W/m}^2$ ). Both these studies used a first-order approximation (Eq. (1)) to assess the TOA direct radiative effect (DRE). While this research provides an interesting starting point in understanding the radiative impacts of aerosols in the SE U.S., it only provides a snapshot of summertime conditions as shown by the calculated value of TOA DRE. To date, there have been over 10 years of satellite data from Terra that can now be used to assess how regional TOA aerosol DRE responds over the longer time period. Since we are not comparing our results to preindustrial levels and we do not attempt to separate anthropogenic and natural sources of aerosols, DRE is the appropriate parameter to estimate as opposed to using direct aerosol radiative forcing (DARF).<sup>4</sup>

The first-order approximation of DRE at the TOA can be defined as adapted by Haywood and Shine<sup>5</sup>:

$$\Delta F = -DS_0 T_{\text{atm}}^2 (1 - A_c) \omega_0 \beta AOD \left( (1 - R_s)^2 - \frac{2R_s}{\beta} \left( \frac{1}{\omega_0} - 1 \right) \right) \quad (1)$$

where  $D$  is the fractional day length, solar constant ( $S_0$ ) =  $1370 \text{ W/m}^2$ ,  $T_{\text{atm}}$  is the atmospheric transmission,  $A_c$  is the fractional cloud amount,  $\omega_0$  is the single-scattering albedo (SSA),  $\beta$  is the up-scatter fraction, and  $R_s$  is the surface reflectance. Goldstein et al<sup>3</sup> only considered changes in AOD by keeping the other variables constant. An SSA of 0.972 was used as a representative value of the optical properties of aerosols in the SE U.S. Also, they chose to use a fixed surface albedo value of 0.15 and fractional cloud cover amount of 0.6 to be representative of the region. Many of these variables can now be measured by satellite, which provides a unique opportunity to assess the TOA radiative effect of aerosols, taking into account the decadal variations in aerosol AOD, cloud fraction, and surface albedo. The National Research Council Report<sup>6</sup> advocates for the better understanding of regional variations in the radiative forcing as well as for long-term monitoring of radiative forcing variables.<sup>4,7,8</sup>

Recent published work used radiative transfer modeling to estimate DRE over various time and geographical scales. For instance, Heald et al<sup>4</sup> used a global chemical transport model with a radiative transfer model to contrast differences between DRE and DARF on a global scale by accounting for decreases in anthropogenic emissions in the future. Whereas Sena and Artaxo<sup>7</sup> used satellite observations of aerosols and fluxes as inputs to a radiative transfer model to estimate DARF associated with biomass burning over Amazonia, which builds upon the methodologies by Patadia et al<sup>9</sup> and Sena et al.<sup>10</sup> Similarly, Sundström et al<sup>8</sup> provided an approach to use satellite-based aerosol DRE in comparison with model-simulated estimates of aerosol DRE. We choose to approach estimating DRE from a more simplistic perspective, and by doing so, we will lay the foundation for future research avenues that will be

comparative of satellite-based estimates of DRE and modeled estimates of DRE for the SE U.S.

Goldstein et al<sup>3</sup> suggested that the negative TOA radiative effect produces cooling at the surface. Earlier analysis of surface temperature using the Goddard Institute for Space Studies (GISS) global climate model suggested that the SE U.S. had cooled over the past hundred years.<sup>11</sup> However, recent reanalysis of surface temperature records point toward a different conclusion, namely, that the Southeast has neither warmed nor cooled.<sup>12</sup> If the latter is accurate, then the implications on whether the haze that persists in the Southeast are indeed responsible for cooling as Goldstein et al hypothesized.

In the study by Alston et al,<sup>13</sup> our analysis of 10 year's of data has revealed distinct seasonality and interannual variations with respect to aerosol concentration and AOD. Building on our previous work, this study seeks to assess the regional TOA DRE and its dynamics over the past decade in the SE U.S. by taking into account changes in cloud cover, surface albedo, and aerosol loading through AOD. We used AOD from MODIS and MISR, cloud fraction from MODIS, and surface albedo data from MODIS from March 2000 to December 2011. Our analysis focuses on determining seasonal and interannual variations of these variables across the region of interest and associated dynamics of DRE, especially the presence of trends. This paper is organized as follows: "Data and methodology" section describes the types of data and methodologies used in this study, "Results" section presents the results of the DRE assessment, and finally, "Conclusions" section gives a summary of major findings.

## Data and Methodology

This research utilizes aerosol products from MODIS and MISR along with cloud fraction and surface land albedo from MODIS. We used Collection 5 Level 2 over land aerosol product MOD04 from MODIS. Please see Refs. 14 and 15 for more information on MODIS aerosol data products. Level 2 data are separated into five-minute granules. One variable of interest to this study is "Optical\_Depth\_Land\_and\_Ocean", which is retrieved at 550 nm. This product combines the corrected optical depth over land and ocean with the best data quality (QA Confidence flag = 3).

MISR AOD used in this analysis is version 22 Level 2 aerosol data, which has a 17.6 km resolution at nadir.<sup>16,17</sup> The AOD values used are "best-estimate AOD" at MISR green (558 nm) band. In their standard product, MISR also has a variable that estimates SSA ( $\omega_0$ ) in the MISR green band, which is used in this analysis.

This study uses a  $5^\circ \times 5^\circ$  latitude/longitude box centered over the SE U.S. The box's coordinates are  $30.5^\circ\text{N}$ – $35.5^\circ\text{N}$  and  $81^\circ\text{W}$ – $86^\circ\text{W}$ . The AOD values associated with the pixels contained within the box are averaged together for each day from March 1, 2000, to December 31, 2011. The daily AOD means are then averaged to create monthly means. MODIS data were obtained from NASA Goddard Space

Flight Center's LAADS (Level 1 and Atmosphere Archive and Distribution System), and MISR data were obtained from NASA Langley Research Center's Atmospheric Data Center.

We also used the same MODIS product (MOD04) to obtain cloud cover information. Specifically, the "Cloud\_Fraction\_Land" subset was selected for our analysis. Cloud fraction is defined as the ratio of the number of cloudy/probably cloudy pixels to the total number of pixels within a granule during the cloud-top algorithm processing.<sup>18</sup> The final dataset used in this analysis is a Level 3 Climate Modeling Grid surface albedo product (MCD43C3) at  $0.5^\circ \times 0.5^\circ$  resolution provided by Dr. Schaaf (personal communication). Albedo is a measure of a surface reflectivity that depends on the surface type. MCD43C3 is a combined product that uses both MODIS sensors, ie, MODIS Terra and MODIS Aqua, as inputs. This product is available in 16-day aggregates every 8 days, which results in a maximum of 46 albedo measurements over a year. Data from MODIS onboard Aqua are not used in this study due to the shorter data record as Aqua was launched in 2002, and it allows us to compare Terra-based instruments exclusively.

The MODIS Albedo products are generated using the Ross-Thick/Li-Sparse-Reciprocal BRDF model.<sup>19</sup> The model parameters are estimated independently for each gridded pixel location by inversion against the MODIS observations (surface reflectance and solar and viewing geometry values) retrieved in the 16-day retrieval period.<sup>20</sup> For more detailed explanation of the Albedo/BRDF algorithm, see Ref. 20. The Albedo product is provided in three broadbands: visible (0.3–0.7  $\mu\text{m}$ ), near-infrared (0.7–5.0  $\mu\text{m}$ ), and shortwave (0.3–5.0  $\mu\text{m}$ ) using the spectral to broadband conversion approach developed by Liang et al.<sup>21</sup> The use of quality flags is necessary to ensure that the albedo values have real meaning with high confidence as to the validity of the values. The confidence associated with the inversion results is provided through the use of data quality flags. This study utilizes the shortwave broadband white sky (isotropic diffuse radiation) albedos, where more than 80% of the albedos values are considered to be acceptable (data flag 2 or lower). Additionally, the 46 files are averaged on a monthly basis with each month having 3–4 retrievals.

TOA DRE is computed using Eq. (1). The methodology is as follows. The area-averaged variables described above are used in the time series analysis and as input in Eq. (1). The analysis of the TOA DRE includes assessments of the effect of cloud fraction and surface albedo on DRE and a combined assessment where AOD, cloud fraction, and surface albedo all change with time. In addition, we examine the effect of SSA ( $\omega_0$ ) on DRE. Finally, we also conduct regional analysis of DRE based on seasonally averaged variables (AOD, cloud fraction, surface albedo, and SSA) on a  $0.2^\circ \times 0.2^\circ$  grid (except surface albedo, which is already globally gridded) over the past 12 years.

For our purposes, we will use the term "cooler" months to refer to winter and fall seasons and "warmer" to refer to spring

and summer. Additionally, we define winter = December (from the previous year)–February; spring = March–May; summer = June–August; and fall = September–November.

## Results

**Analysis of temporal variability of AOD, cloud fraction, and surface albedo.** Our analysis revealed strong seasonality in the satellite AOD datasets of MODIS and MISR. During the summer months, average AOD increases two to three times from winter AOD averages for both instruments.<sup>13</sup> This seasonality is prominently displayed in the seasonally averaged maps of AOD for both MODIS and MISR shown in Figure 6 of our earlier work Ref. 13. Figure 1 shows the MODIS and MISR satellite monthly mean AOD as a time series from 2000 until 2011. Maxima occur during the warmer months with minima occurring during the cooler months. For most years, the maxima occur near 0.4, but in more recent years, the maxima are around 0.3, whereas the minima hover between 0.05 and 0.1. In 2007, there is an increase in AOD, which is primarily driven by increased aerosol loading due to wildfire activity during the late spring and early summer.<sup>22</sup> For instance, the elevated values of AOD from both sensors in 2007 corresponded to increases in surface-level measurements of fine particulate matter.<sup>13</sup> Alston et al<sup>13</sup> provided more in-depth analysis of AOD and surface-level particulate matter.

Overall both datasets have decreasing trends with time. To determine trends without seasonal basis, the same methodology from the study by Alston et al<sup>13</sup> is used. Briefly, the 12-year monthly average is calculated and then subtracted from each respective month, thus creating a time series of anomalies. It is these anomalies that are used to assess the trends without a seasonal bias. MODIS has a statistically significant decreasing linear trend (slope =  $-0.000415$ ) in the monthly AOD anomalies using a  $t$ -test for  $\alpha = 0.05$ .

The time series of cloud fraction does not appear to have an overall trend. As shown in Figure 2, cloud fraction appears to have a bimodal behavior in terms of maxima. The summer months generally have the highest maxima, and the winter months also have maxima albeit lower than the summer maxima. The largest minima occur during the fall with the spring having the other minima. Minima values vary around 0.2–0.45, while maxima values vary between 0.5 and 0.8. Additionally, the shorter time period considered in this study makes detecting a linear trend within the record challenging. As such, there is not a discernable trend in the monthly anomalies of cloud fraction.

Our analysis of surface albedo revealed the distinct seasonality as shown in Figure 3. As expected during the warmer seasons, there are albedo changes associated with a green-up of vegetation that results in seasonal maxima. While there is a seasonal cycle, the southeastern region of the U.S. is a region that stays green throughout the year due to high concentration of evergreen trees. Interestingly, during the first seven years of the time series, the maxima are almost 0.155, yet during the

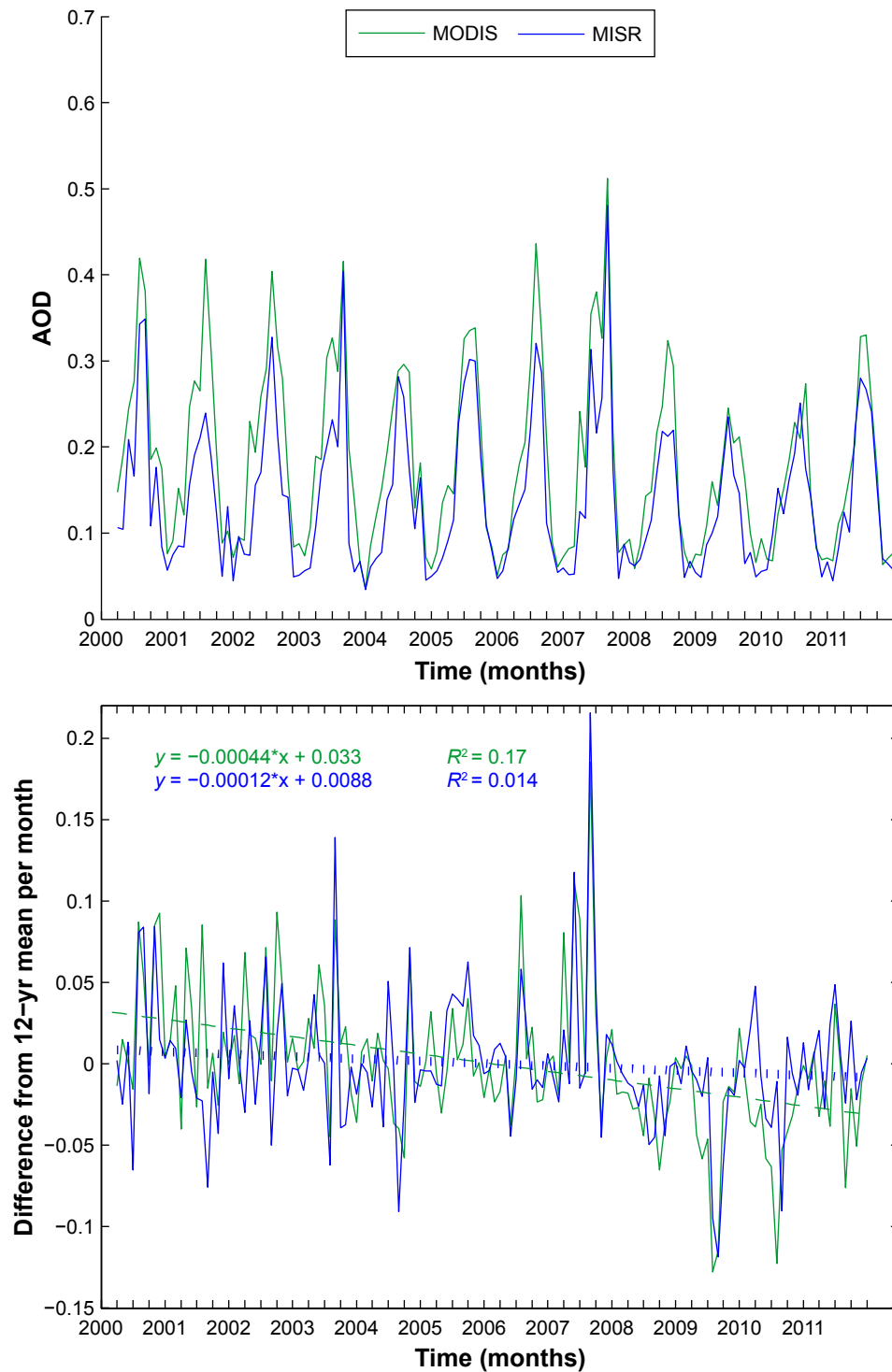


**Figure 1.** (Top) Time series of monthly mean AOD from MODIS and MISR. (Bottom) Time series of monthly mean AOD anomalies from MODIS and MISR. Linear regression information inset with figure.

**Note:** \*Notation refer to Pg. 9.

latter years, the maxima only occurs between 0.145 and 0.15. Barnes and Roy<sup>23</sup> found that this region experienced over a 20% change in land cover and land use from 1973 to 2008, though the associated albedo change during that time was negligible because the region retained a forested type of ecosystem. Subsequently, our area-averaged albedo values compare well with those of the study by Barnes and Roy.<sup>23</sup> The minima

occur between 0.1175 and 0.13, but the minima appear to be declining over time as well. After removing the seasonal component, we found that surface albedo monthly anomalies have a decreasing linear trend (slope =  $-0.000052$ ) for  $\alpha = 0.05$ .

#### Assessment of the aerosol DRE.

*Time series analysis of aerosol DRE.* Allowing the AOD, cloud fraction, and surface albedo to vary with time is more

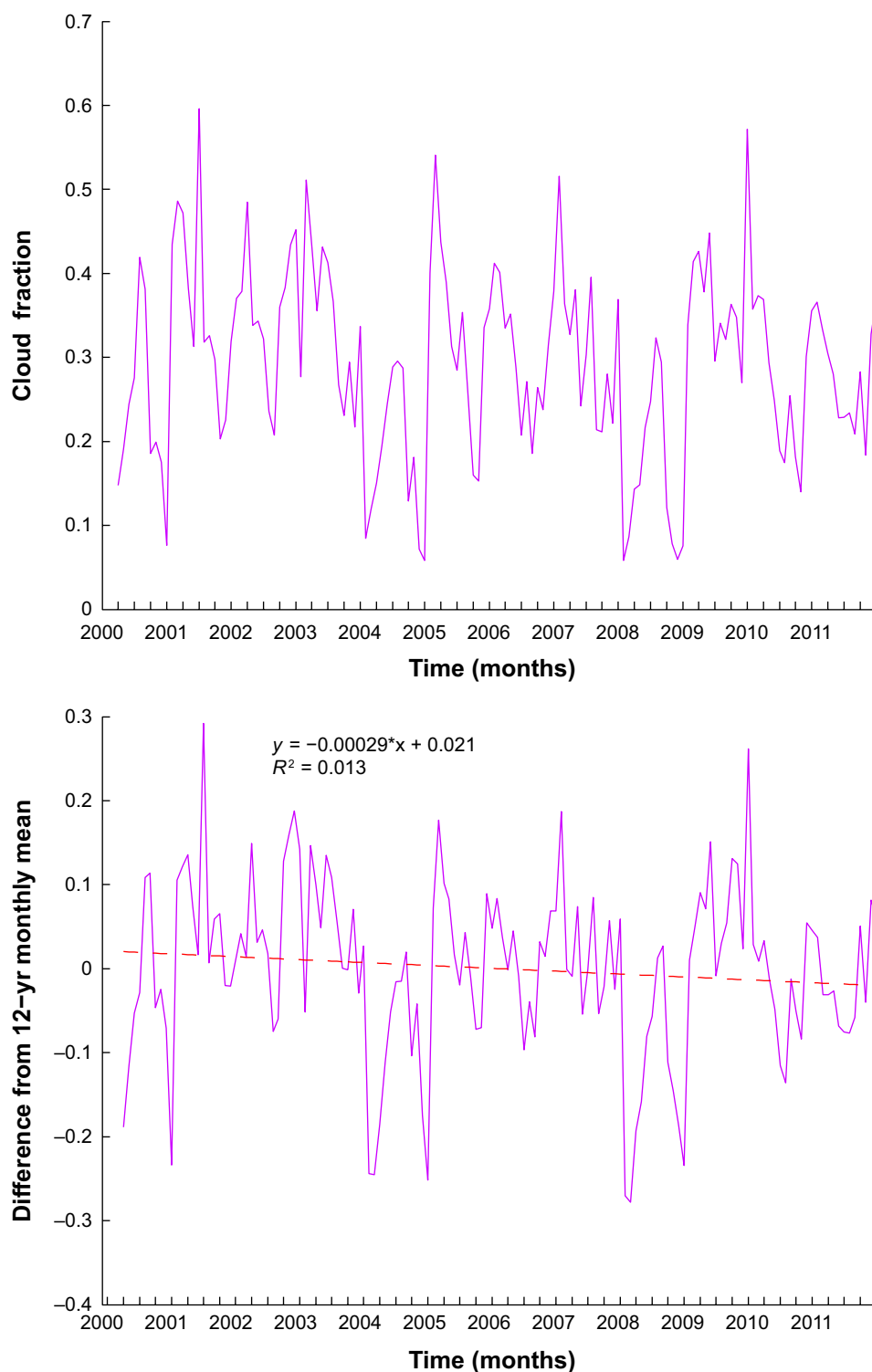


**Figure 2.** (Top) Time series of monthly mean cloud fraction. (Bottom) Time series of monthly mean cloud fraction anomalies. Linear regression information inset with figure.

**Note:** \*Notation refer to Pg. 9.

reflective of actual variations in atmospheric and environmental conditions. We also allow the fractional day length (denoted as  $D$ ) in Eq. (1) to vary with time according to the latitude in Atlanta as a representative value of day length for the entire region. To make comparisons with other published references, we adopt an  $SSA = 0.972$  only for this section's analysis.

The behavior of the DRE estimates in Figure 4 appears similar for both satellite instruments.

In Figure 4, the DRE broadly resembles the behavior of the AOD. Closer examinations of the periods of increased negative DRE ( $DRE \leq -15$ ) generally occur during periods of wildfire activity. It is likely that these high AOD events

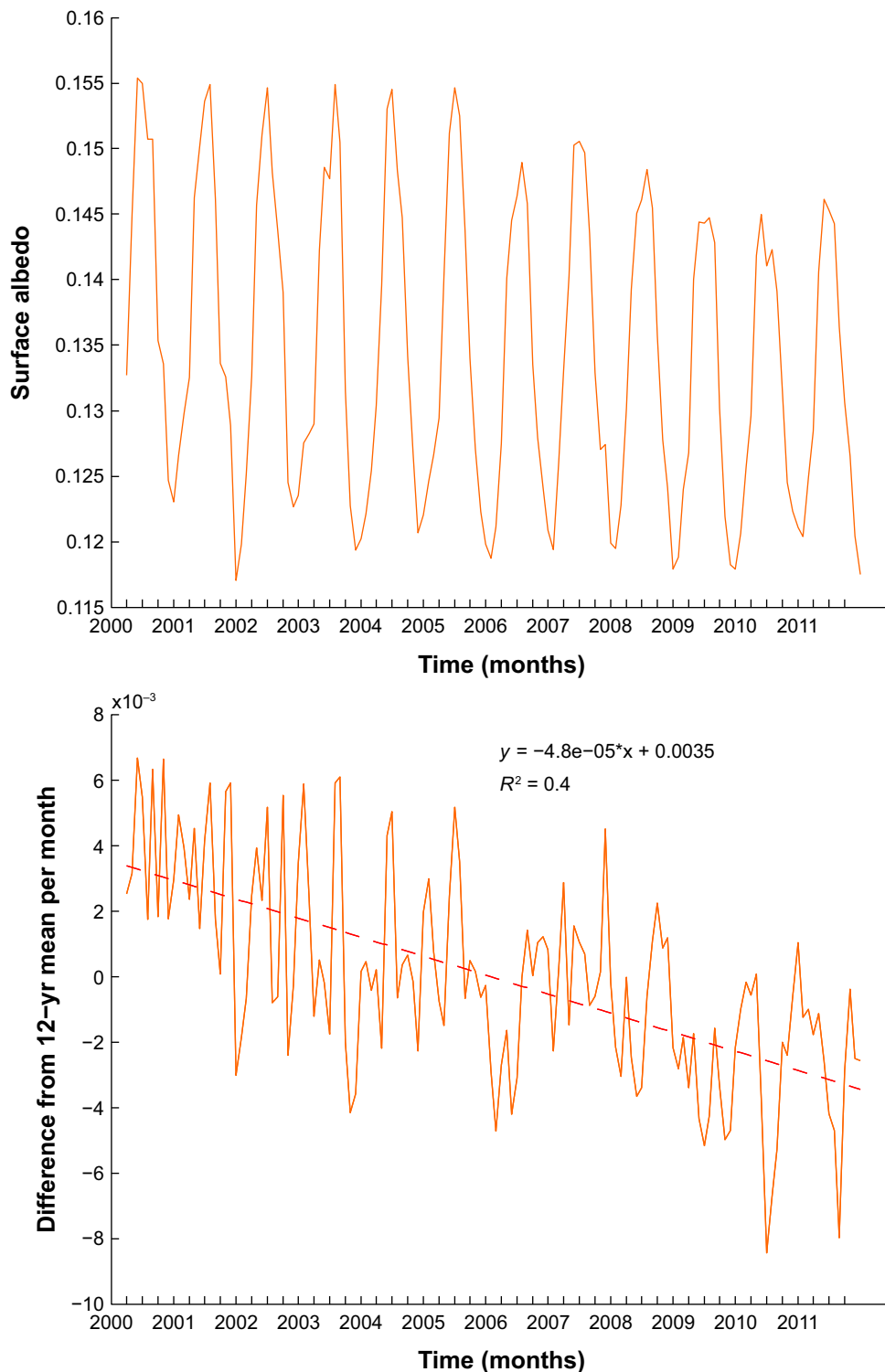


**Figure 3.** (Top) Time series of monthly mean surface albedo. (Bottom) Time series of monthly mean surface albedo anomalies. Linear regression information inset with figure.

**Note:** \*Notation refer to Pg. 9.

and weather dynamics (eg, high-pressure systems that increase aerosol loading that take place during the summer) increase the standard deviation (STD) of the AOD and thus the estimated DRE. Given the seasonality within the time series, we performed the STD calculation on each respective month over all 12 years, eg, all Januaries were combined to calculate

the STD of the estimated DRE for January and so on. The monthly mean (12-year mean of each respective month) of DRE from MODIS during January is  $-2.47 \pm 0.351 \text{ W/m}^2$  and during July is  $-15.74 \pm 3.71 \text{ W/m}^2$ . During January, the mean for MISR is  $-1.8 \pm 0.55 \text{ W/m}^2$ , and during July, the mean is  $-12.11 \pm 3.05 \text{ W/m}^2$ .

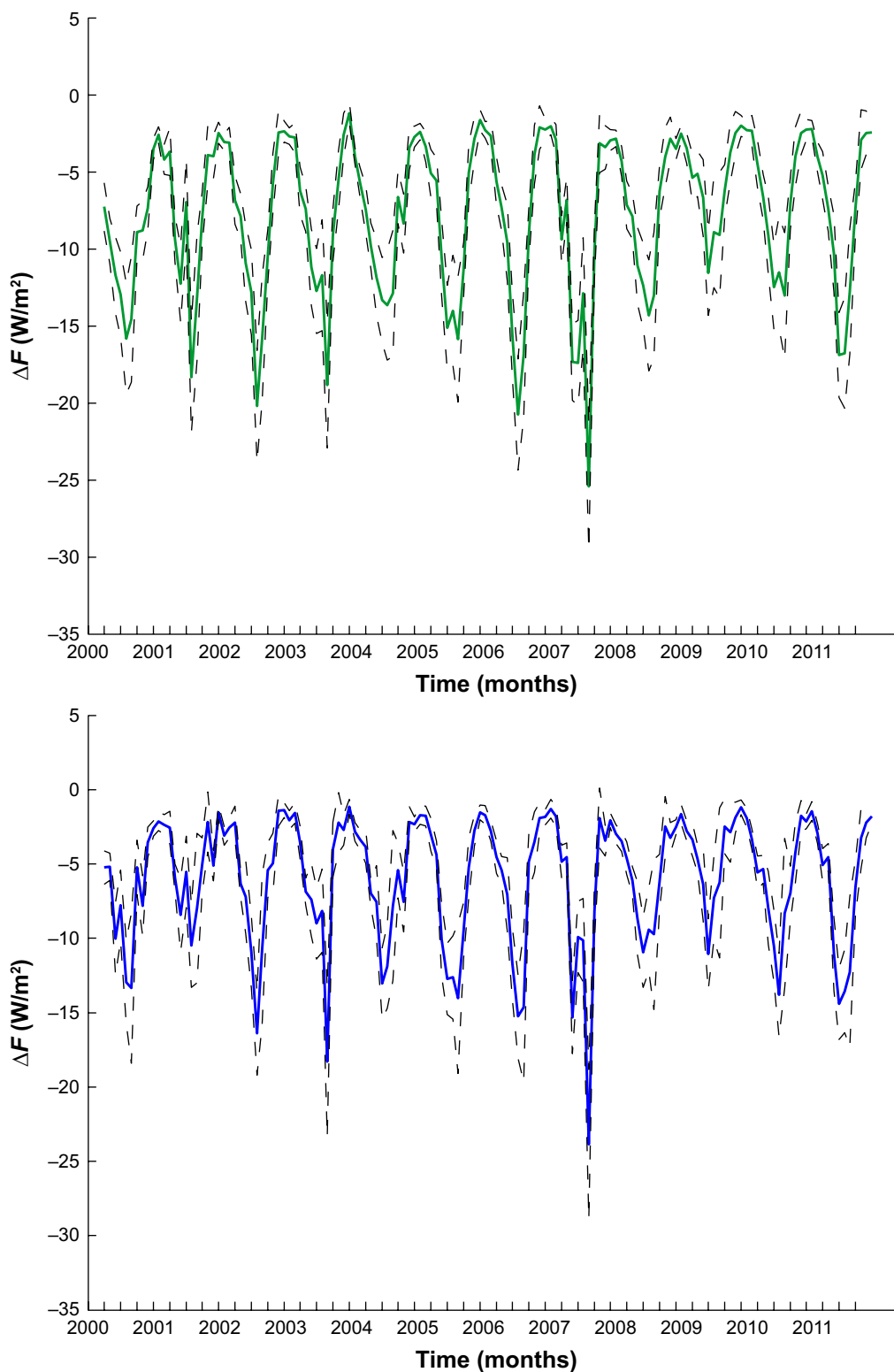


**Figure 4.** (Top) Time series of estimated DRE based on MODIS AOD, cloud fraction, and surface albedo. (Bottom) Time series of estimated DRE based on MISR AOD, cloud fraction, and surface albedo. The dashed black line represents  $\pm$  the STD of the estimated DRE.

To further examine the seasonality within the DRE calculations, we calculated differences between the estimated DRE from MODIS and the estimated DRE from MISR using the same variables used in the calculations in Figure 5 (Table 1). From a seasonal perspective, we observe that the relative

differences between the two estimates of DRE increases during heavier aerosol loading seasons (Spring and Summer) with smaller relative differences occurring during the fall and winter. We also recognize that the difference in aerosol composition drives some of the observed difference in DRE as well.



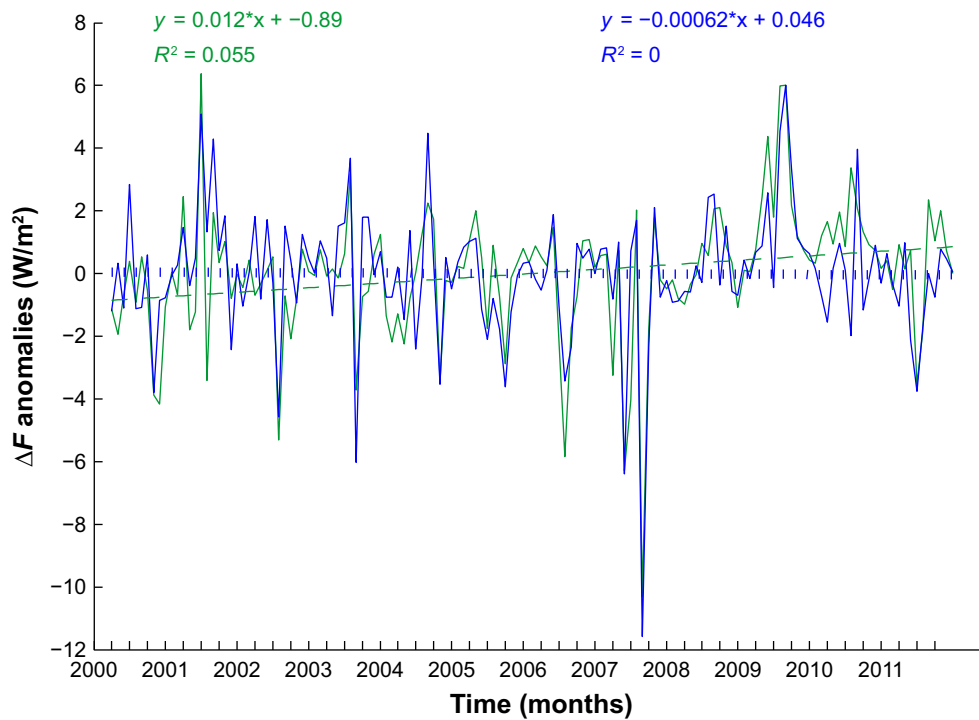


**Figure 5.** Time series of monthly anomalies of DRE based on AOD for both MODIS (green) and MISR (blue).  
**Note:** \*Notation refer to Pg. 9.

During the cooler months, the minima (less negative) of DRE vary between  $-6$  and  $-3$   $W/m^2$ , and during the warmer months, there is more variation with the range of  $\Delta F$  varying between  $-24$  and  $-12.6$   $W/m^2$  for MODIS and  $-22.5$  and  $-11$   $W/m^2$  for MISR. Yet if we take an average over time, ie, over 142 months—due to Terra spacecraft launch in January 2000 with complete data records beginning in March 2000, this yields  $\Delta F = -7.57$   $W/m^2$  for MODIS and  $\Delta F = -5.72$   $W/m^2$  for MISR. The estimates of DRE presented

here are more negative compared with the results by Carrico et al,<sup>2</sup> where they used the same first-order approximation to estimate forcing ( $\Delta F = -11.6 \pm 6$   $W/m^2$ ) using instantaneous measurements of optical properties during six weeks in late summer 1999 in Atlanta. The estimates of DRE have a slightly increasing (less negative) linear trend, but it is not statistically significant. To determine if there is a true trend, we use a similar methodology here to calculate monthly radiative DRE anomalies by removing the seasonal signal from the time series

**Table 1.** Seasonal differences in DRE.

MONTH	YEAR											
	2000	2001	2002	2003	2004	2005	2006	2007	2008	2009	2010	2011
December	0.000	-0.453	0.042	-0.618	-1.133	-0.687	-0.560	-0.749	0.154	-0.880	-0.397	-0.761
January	0.000	-1.828	-0.532	-1.192	-2.322	-1.592	0.141	-1.105	-0.847	-0.698	0.992	-1.072
February	0.000	-0.890	-0.928	-0.987	-0.039	-0.389	-0.118	-0.387	-0.861	-0.985	-0.813	-0.131
March	-2.015	-1.135	-4.591	-2.679	-3.579	-2.070	-1.061	-4.507	-2.511	-2.015	1.072	-0.166
April	-4.259	-3.408	-1.539	-0.542	-2.777	-1.141	-1.887	-2.274	-1.758	-0.477	-1.253	-2.852
May	-1.682	-3.797	-3.696	-3.755	-4.235	-0.462	-2.520	-2.007	-2.398	-0.326	-1.122	0.739
June	-5.115	-1.421	-1.862	-3.683	-0.296	-2.360	-3.855	-7.425	-1.447	-0.468	-1.953	-2.463
July	-2.864	-7.744	-3.775	-3.539	-1.726	-1.375	-5.449	-2.714	-4.883	-1.618	2.260	-3.179
August	-1.220	-5.150	-5.027	-0.517	-5.019	-1.787	-2.200	-1.555	-3.272	-2.803	-4.694	-0.496
September	-3.664	-2.939	-5.012	-5.048	-1.202	-1.820	-4.226	-1.964	-0.077	-3.728	-0.077	-0.769
October	-0.972	-1.700	-0.778	-3.247	-0.794	0.166	-0.331	-1.229	-1.533	-0.832	0.201	0.329
November	-3.813	1.097	-1.007	0.105	-1.270	-0.117	-0.220	0.010	0.370	-0.606	-0.694	-0.262

**Notes:** Differences are calculated as MODIS DRE—MISR DRE. Positive values = MODIS DRE < MISR DRE. December monthly means are taken from the previous year, eg, Winter 2002 = December 2001–February 2002.

as was used in Ref. 13. We then use the monthly anomalies to fit a linear regression (Fig. 5). The MODIS anomaly time series show an increasing trend with time, which implies decreasing DRE (less negative), which are statistically significant at the 95% confidence level where the slope is  $0.012^*$ . We acknowledge that our calculated trends could be due to detector degradation shifts onboard the MODIS instrument<sup>24</sup> that are found in Collection 5.1 L2 data. As such, we will annotate our trend verbiage with an asterisk (\*). As shown in Figure 1, the MISR AOD time series has less of a discernable trend in comparison to MODIS. While numerous studies have shown good correlation between MODIS and MISR AOD products, there are inherent differences in satellite retrievals, algorithms, spatial scales, etc. that are likely impacting the results shown here. The declining AOD trends with both sensors for this region of the U.S. are in agreement with the recently published work.<sup>25,26</sup> Without the significant decrease in the MISR AOD, it stands to reason that the trend for the DRE for MISR would be near zero, given that we have determined that the primary driver of DRE is AOD.

To better visualize the differences between the estimated DRE based on AOD (Fig. 5) from the DRE calculated using AOD, cloud fraction, and surface albedo (Fig. 4), we subtracted the AOD only estimates with results shown in Figure 6. The convention is as follows: if the AOD only estimates are greater than the combined estimates, then the difference is positive; however, if the AOD only estimates are less than the combined estimates, then the difference is negative.

During the cooler months, the difference is between 1 and 2  $W/m^2$ , which implies that the addition of surface-cloud effects reduces the estimated DRE during this time period. Not surprisingly, the largest difference was noted in the warmer months, where the differences varied between  $-7$  and  $-3$   $W/m^2$ . The aerosol-cloud effects appear to have an additive effect on the DRE, especially during periods of high AOD (increased negative DRE).

*Regional assessment of aerosol DRE.* A primary goal of this research is to better understand the regional nature of aerosol DRE. The SE U.S. is a large region, and area-averaged results as have been shown previously in this work because these analyses are useful in drawing general conclusions. However, it does not show how the region as a whole responds to aerosol radiative effects. The following analysis will use the same satellite variables to assess DRE on a regional basis. Figure 7 shows the regionally averaged July DRE using both satellite instruments as input. AOD and SSA regional distributions primarily drive the variations of DRE. The more industrialized areas with increased concentrations of aerosols show in contrast to the remainder of the region's background levels of DRE of  $\sim -12$   $W/m^2$ . The increased DRE in the industrialized areas could be indicative of increased anthropogenic factors.

#### Sensitivity case studies.

*Effect of cloud fraction and surface albedo on aerosol DRE.* Functional analysis of Eq. (1) provides some useful insight

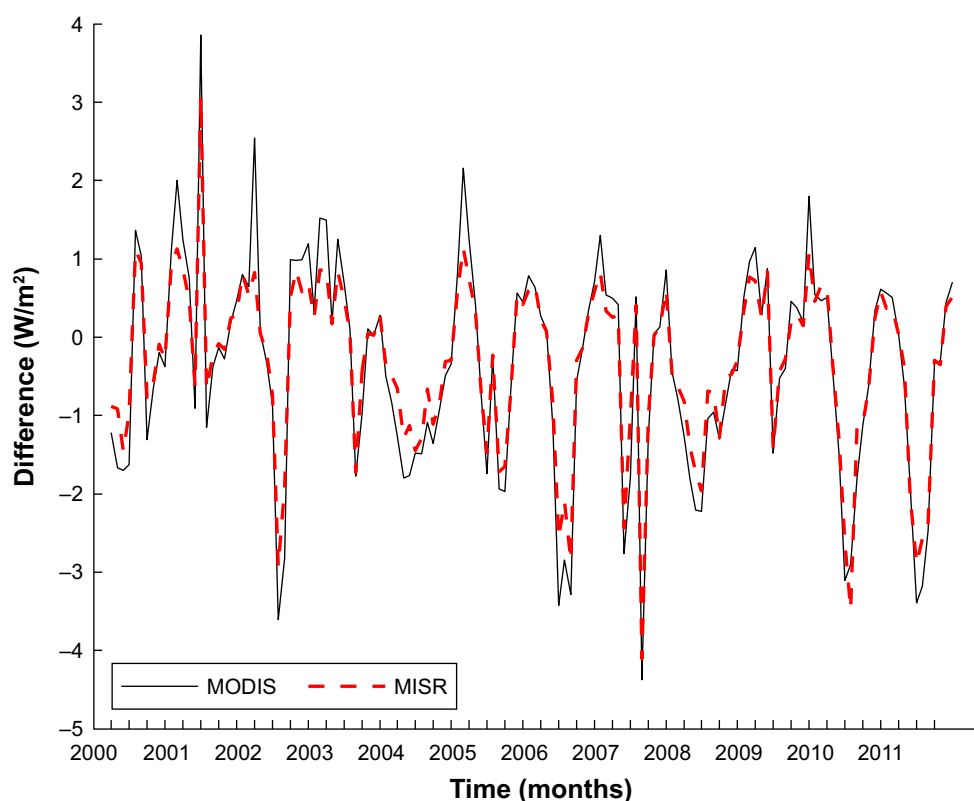


**Figure 6.** Time series of the difference in DRE where difference = DRE due to AOD, cloud fraction, and surface albedo—DRE due to only AOD.

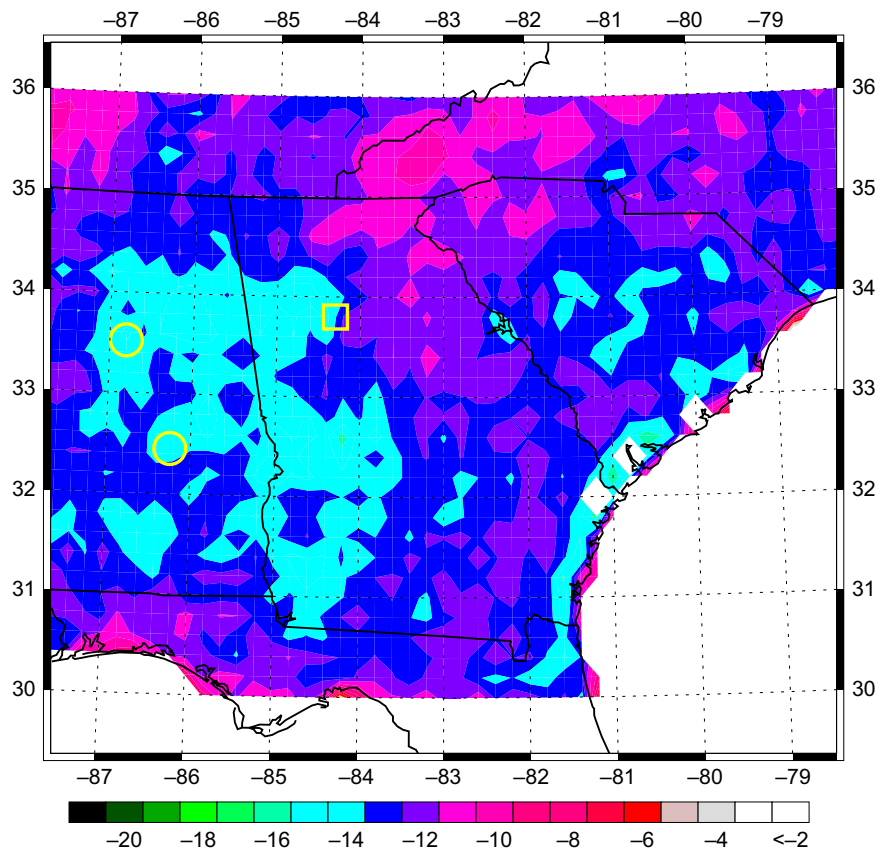


**Figure 7.** Regional assessment of DRE at the TOA based on monthly mean MODIS AOD, MISR SSA, MODIS surface albedo, and cloud cover for July 2000–2011. The yellow symbols are representing large industrial areas: square = Atlanta, GA, and circles = Birmingham, AL, and Montgomery, AL.

into the main drivers of DRE. Yet the time series analysis revealed that cloud fraction varies the most with time, which could influence the behavior of the estimated DRE. As discussed in “Introduction” section, for these calculations of TOA radiative effect, means of the variables are calculated for use in lieu of representative values along with the other equation constants; thus, to assess the influence of each variable, only this variable is allowed to vary with time.

Estimated DRE considering variations in surface albedo and cloud fraction is shown in Figure 8, and the estimated DRE only considering varying AOD (MODIS and MISR) is shown in Figure 9. Not surprisingly, the estimated DRE closely resembles the behavior of the input variables. The range of estimated TOA radiative effect ( $\Delta F = -8.14$  to  $-7.68$   $\text{W/m}^2$ ) only due to surface albedo varied the least. The range of  $\Delta F$  varied between  $-8.9$  and  $-4.5$   $\text{W/m}^2$  due to cloud fraction. Only considering AOD variations yielded the largest range in  $\Delta F$  ( $-19$  to  $-3.3$   $\text{W/m}^2$ ) for MODIS. Using a time series of input data allows for understanding the dynamic nature of the radiative effect associated with changes in aerosols and other time-varying factors, instead of simplifying it down to a single summertime value as was done in the study by Goldstein et al<sup>3</sup> ( $\Delta F = -3.9$   $\text{W/m}^2$ ).

Estimates of TOA aerosol radiative effect are modulated by variations of other time-dependent variables. How these

estimates respond to only non-aerosol (non-AOD) variations are shown in Figure 10. In Figure 10, we compare our approach of estimating DRE using all satellite data inputs with regionally averaged constants calculated from the satellite datasets. Each month DRE is averaged across the time period of 12 years to provide a January average, etc. While AOD is the primary driver of DRE, cloud fraction and surface albedo have modulating effects, which results in all values being similar. During the warmer months, the baseline case (all satellite datasets vary with time) appears to slightly underestimate DRE when compared with the cooler months. The inherent seasonal changes are lost when constant values are used. From Figure 11, we compare January and July DRE and find a difference of  $\sim -13$   $\text{W/m}^2$ . Given the dynamics of cloud fraction, surface albedo, and AOD, our results seem to suggest that by using observations to estimate DRE instead of averaged values yields a more complete perspective of the climatic system.

*Effect of SSA on the aerosol DRE.* Seasonal differences in aerosols not only affect concentration but also composition. A spatial analysis was performed using SSA from MISR averaged over 2000–2011 to better understand the effect seasonality had on aerosol composition (Fig. 11). Both seasons appear fairly uniform, though during the winter MISR had some retrieval errors. SSA ranges from as low as  $\sim 0.87$  to as

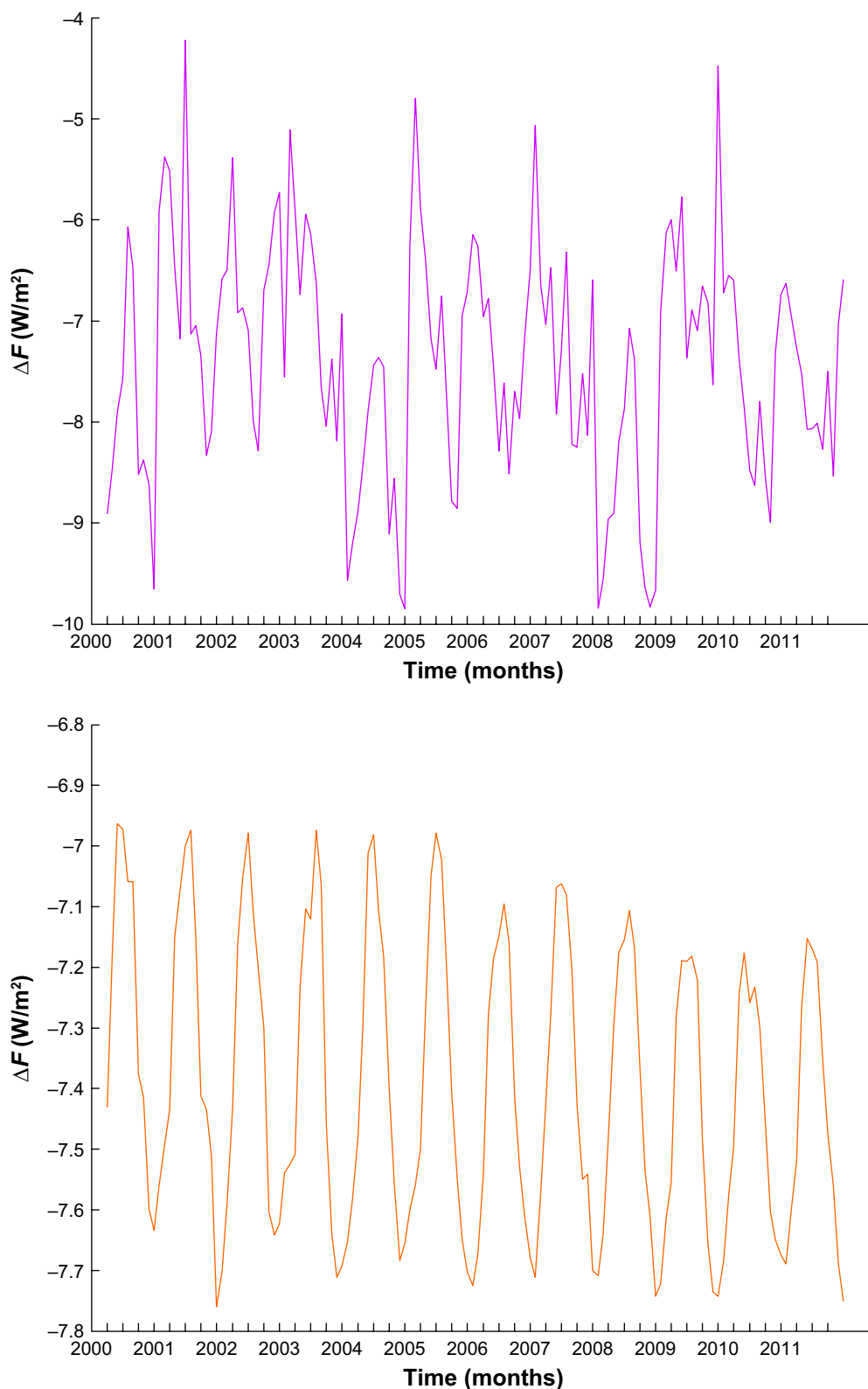


**Figure 8.** (Top) Time series of estimated TOA radiative effect due to only cloud fraction. (Bottom) Time series of estimated TOA radiative effect due to only surface albedo.

high as 0.96. The adopted average SSA of 0.972 used in “Time series analysis of aerosol DRE” section is slightly higher than observed in this analysis. However, the use of this averaged SSA is unlikely to lead to large errors, given the uniformity

of SSA in the region (Fig. 11) and the relative closeness of the averaged SSA and the SSA observations. This conclusion allows for this analysis to be taken in the context of other similar studies.

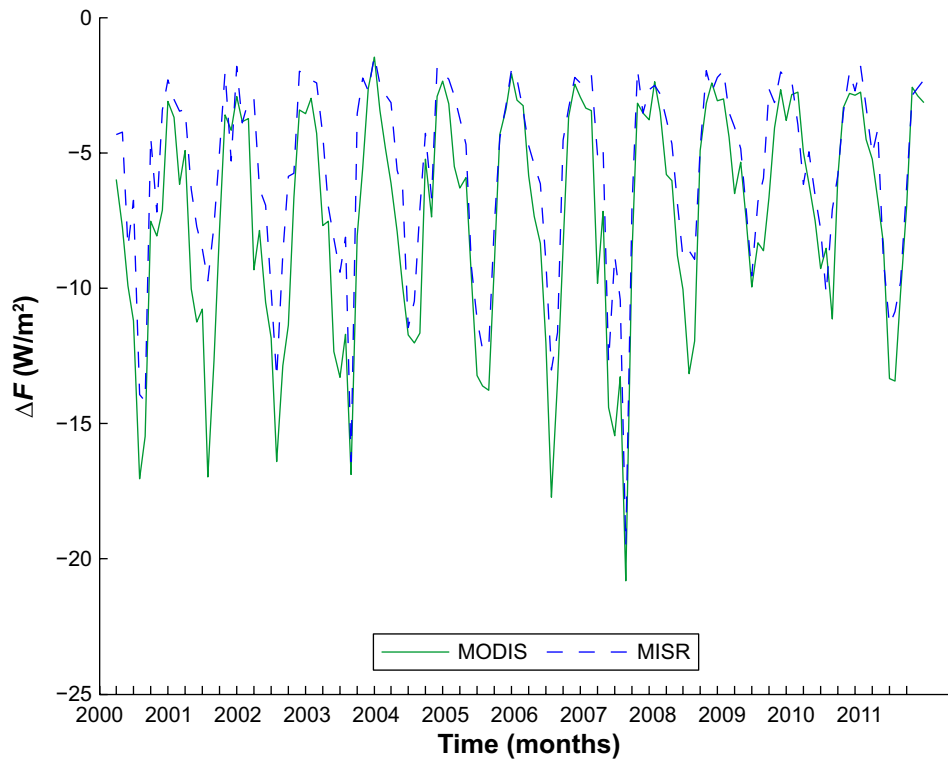


**Figure 9.** Time series of estimated radiative effect based on AOD from MODIS and MISR.

The three SSAs used are 0.8, 0.85, and 0.9, which are more consistent with measurements of SSA in the region,<sup>2</sup> recalling that all previous estimates used a high SSA of 0.972, eg, the study by Goldstein et al.<sup>3</sup> We estimated TOA  $\Delta F$  due to AOD, cloud fraction, and surface albedo along with varying

SSA (Fig. 12). The lower SSA results in less negative DRE that is most notable during the summer months. For instance, for SSA = 0.8, the largest maxima (most negative) value of DRE is approximately  $-19 \text{ W/m}^2$  for MODIS and  $-18 \text{ W/m}^2$  for MISR. Whereas for higher SSA shown earlier in this analysis,

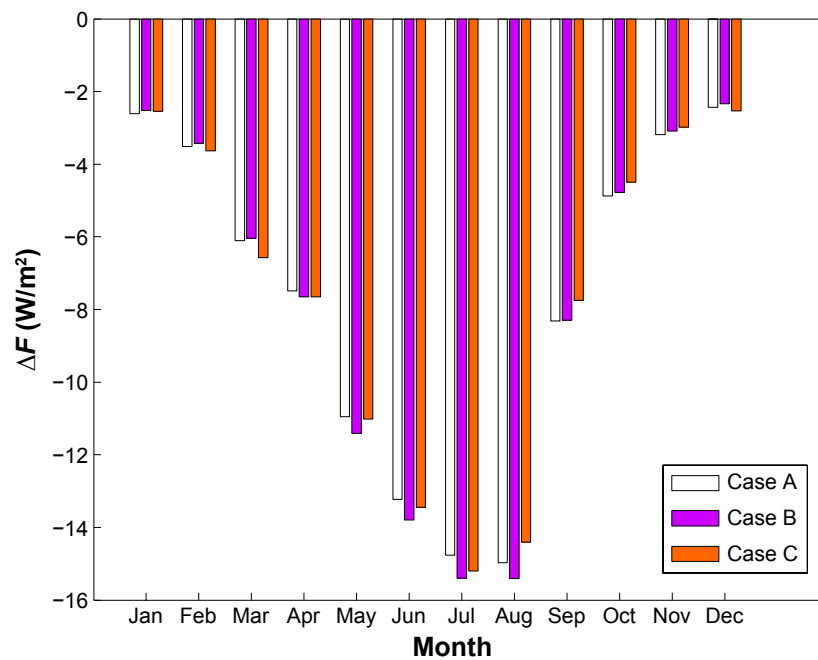


**Figure 10.** Monthly averages of DRE. Case A = all satellite datasets vary with time; Case B = AOD and cloud fraction vary with time; Case C = AOD and surface albedo vary with time.

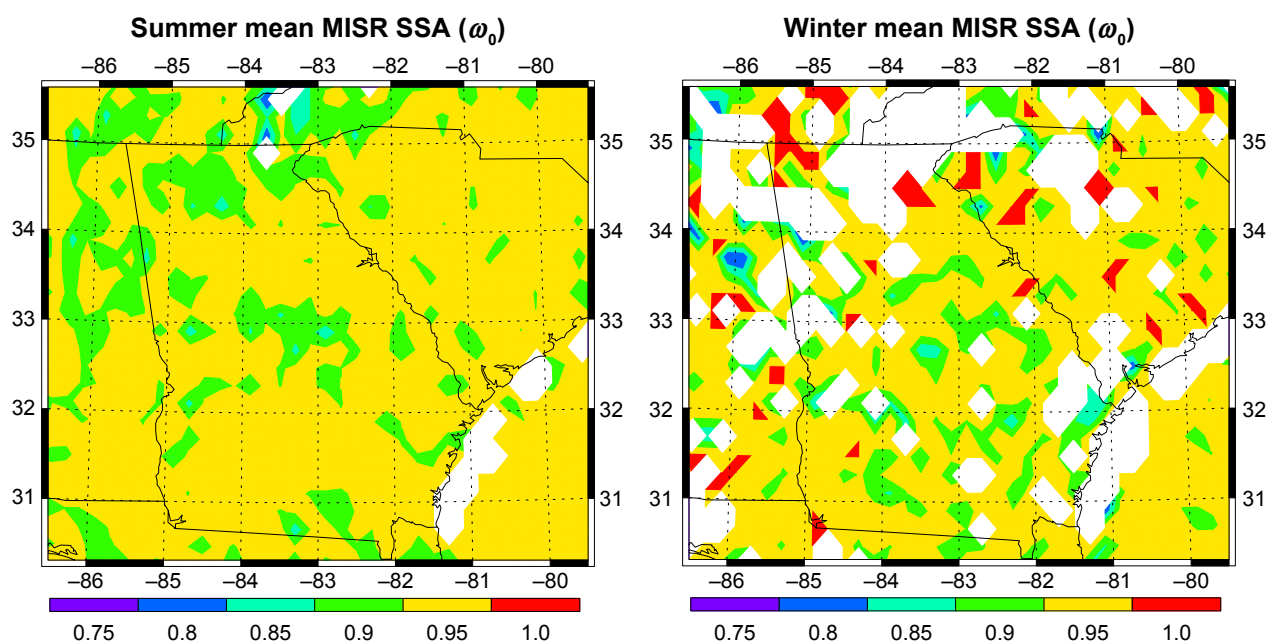


**Figure 11.** Maps of satellite derived winter and summer mean SSA from MISR onboard Terra for the years 2000–2011.

the largest maxima values were  $\sim -24 \text{ W/m}^2$  and  $-22 \text{ W/m}^2$  for MODIS and MISR, respectively. Yet, for the cooler months when the DRE is at a minimum, varying SSA has little effect. If SSA fluctuated more (possibly due to the influx of different aerosols, eg, smoke) for this region, then it is possible that it would have a more pronounced effect on the estimates of DRE at the TOA.

To sum up major points of this analysis, first we have shown that using average values for AOD, cloud fraction, surface albedo, and SSA causes the seasonal characteristics to be lost in the TOA DRE estimates. Our analysis showed that incorporating seasonal variations leads to a more robust representation of DRE for this region. During the summer, TOA DRE can be as large as  $\sim -24 \text{ W/m}^2$  during biomass burning events and on average is  $\sim -16 \text{ W/m}^2$  using MODIS AOD and  $\sim -12 \text{ W/m}^2$  using MISR AOD. Our estimates agree well with results from the study by Carrico et al,<sup>2</sup> which found that instantaneous forcing was  $\sim -12 \text{ W/m}^2$  during the late summer of 1999. However, our results do not agree well with the estimated radiative effect presented in the study by Goldstein et al<sup>3</sup> ( $\sim -4 \text{ W/m}^2$ ), which calculated TOA radiative effect due to summer aerosols, yet our differences due to summer aerosols are almost triple Goldstein's on average.

## Conclusions

The primary goal of this study was to estimate the regional TOA aerosol DRE and its dynamical nature over the past decade in the SE U.S. by accounting for changes in aerosol loading (AOD), cloud cover, and surface albedo. The use of 12-year datasets allows for understanding how these variables and DRE change from a seasonal perspective. By exploring seasonality, differences in aerosol composition and aerosol

concentration can be taken into account. The AOD datasets from MODIS and MISR (both sensors onboard the Terra satellite) have decreasing linear trends. The MODIS AOD linear trend (slope =  $-0.000415$ ) is statistically significant using a  $t$ -test statistic for  $\alpha = 0.05$ . Also, the surface albedo from MODIS shows a statistically significant decreasing linear trend (slope =  $-0.000052$ ) for  $\alpha = 0.05$ , while cloud fraction from MODIS does not have an apparent trend.

Through varying AOD, cloud fraction, and surface albedo one variable at a time while all other variables are kept constant allowed determination of the major drivers of DRE. AOD was a major driver of DRE, while surface albedo and cloud fraction have modulating impacts on the influence of AOD on the DRE. Allowing AOD, surface albedo, and cloud fraction to vary gives a broad range of estimates of DRE from around  $-28$  to  $-3 \text{ W/m}^2$ . During the warmer months, the range of DRE varies between  $-28$  and  $-12.6 \text{ W/m}^2$  for MODIS and  $-26$  and  $-11 \text{ W/m}^2$  for MISR. In comparison, Goldstein et al<sup>3</sup> estimated that the DRE was  $-3.9 \text{ W/m}^2$ . The results of this study suggest that this value is overly simplistic, and it does not provide any insight into the distinct seasonality of the aerosols in the SE U.S. Additionally, these results expand the findings of the study by Alston et al,<sup>13</sup> which suggests that this region is experiencing solar brightening as shown by a slightly increasing linear trend within the DRE dataset.

The results from the SSA analysis provide some interesting connections. SSA of 0.8, 0.85, and 0.9 were considered for all input variables, and during the warmer months, the differences between the DRE estimates based on SSA were pronounced. As expected, higher SSA yielded increased TOA DRE (negative values). An interesting follow on to this work would be to

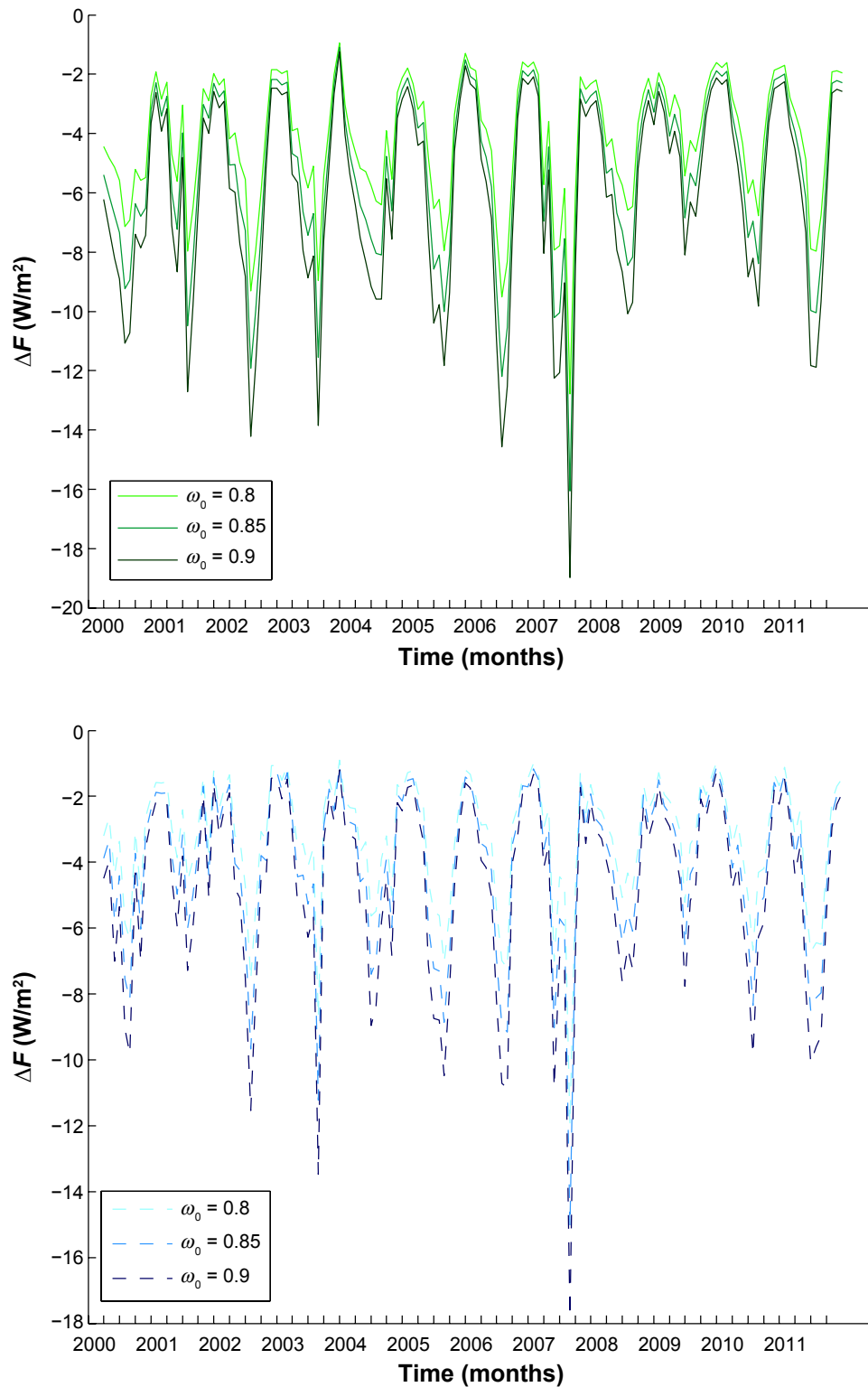


**Figure 12.** (Top) Time series of estimated DRE based on MODIS AOD, cloud fraction, and surface albedo for three different SSA ( $\omega_0$ ) values. (Bottom) Time series of estimated TOA DRE based on MISR AOD, cloud fraction, and surface albedo for three different SSA ( $\omega_0$ ) values.

examine the changes in aerosol composition to provide a better understanding of SSA changes with time. Regional assessment of DRE highlighted the impact that urbanized areas have in comparison to the region's background. Near urban centers, DRE increases ( $\sim -12 \text{ W/m}^2$ ) with respect to background levels.

Our analysis revealed increased AOD associated with wildfires both locally and transported into the region. These smoke aerosols increase AOD, but these aerosols are more light absorbing than sulfate-based aerosols due to increased amounts of black carbon. Over the time period considered



here, the larger wildfires typically occur during the warmer months. If the climate continues to change to a warmer equilibrium, it is possible that the spatial extent and duration of the wildfires will increase, which will ultimately change the concentration and composition of aerosols in this region.

We calculated monthly anomalies of estimated DRE, and we found that with time there is a positive trend\*, which implies that the region is experiencing less radiative cooling, ie, solar brightening. The trend based on estimated DRE for both satellites was positive; however, only the MODIS Terra trend was statistically significant at the 95% confidence interval. It is likely that the driver behind this trend is the reduction of anthropogenic aerosol precursors due to the air quality control policies enacted by the U.S. Environmental Protection Agency (EPA), though it could take decades to detect the measurable reductions with statistical confidence.<sup>27</sup> For the sake of argument, assuming that the anthropogenic portion of SOA can be regulated and reduced, the natural emissions of aerosols could respond to the increased surface temperature by outputting either more or less biogenic aerosols. Unless the biogenic sources emit more than the reduced anthropogenic sources, then it could result in a net reduction of aerosols aloft, ie, less “protective” cooling effects of aerosols at the TOA. Interestingly, Carlton et al<sup>28</sup> posited that biogenic SOA precursors can be regulated as well. In fact, Portmann et al<sup>29</sup> posited that changes in vegetation in the region have had climatic impacts in precipitation and temperature. Hansen et al<sup>30</sup> suggested that the climate has shifted into more extreme warm events, especially during the summertime. Combined regulations and climatic changes will have a direct impact upon SOA production and behavior, which could have impacts at the TOA and surface by reducing the protective layer aerosols. The term “protective” here means that the aerosols are likely dampening the effects of climate change in the region. One of the implications of this is that future climate for this region may shift in light of additional temperature forcing. Future research could focus upon comparing the results of our 1-D TOA DRE assessment with a radiative transfer model attuned to the SE U.S. as described in Refs. 31 and 32 and make estimates of DARF. This would provide an opportunity to explore future climate scenarios based upon predicted emissions.

### Acknowledgments

The authors would like to thank Dr. Olga Kalashnikova of the Jet Propulsion Laboratory for assistance with the MISR data. We also would like to thank Dr. Crystal Schaaf at Boston University for assistance with the MODIS surface albedo product and its utilization.

### Author Contributions

Conceived and designed the experiments: EJA. Analyzed the data: EJA. Wrote the first draft of the manuscript: EJA. Contributed to the writing of the manuscript: INS. Agreed

with manuscript results and conclusions: EJA and INS. Jointly developed the structure and arguments for the paper: EJA and INS. Made critical revisions and approved the final version: EJA and INS. All the authors reviewed and approved the final manuscript.

### REFERENCES

1. Edgerton ES, Hartsell BE, Saylor RD, Jansen JJ, Hansen DA, Hidy GM. The Southeastern aerosol research and characterization study, part 3: continuous measurements of fine particulate matter mass and composition. *J Air Waste Manag Assoc.* 2006;56(9):1325–1341.
2. Carrico CM, Bergin MH, Xu J, Baumann K, Maring H. Urban aerosol radiative properties: measurements during the 1999 Atlanta supersite experiment. *J Geophys Res Atmos.* 2003;108(D7):8422.
3. Goldstein AH, Koven CD, Heald CL, Fung IY. Biogenic carbon and anthropogenic pollutants combine to form a cooling haze over the southeastern United States. *Proc Natl Acad Sci U S A.* 2009;106:8835–8840.
4. Heald CL, Ridley DA, Kroll JH, et al. Contrasting the direct radiative effect and direct radiative forcing of aerosols. *Atmos Chem Phys.* 2014;14(11):5513–5527.
5. Haywood JM, Shine KP. The effect of anthropogenic sulfate and soot aerosol on the clear sky planetary radiation budget. *Geophys Res Lett.* 1995;22(5):603–606.
6. National Research Council. Radiative Forcing of Climate Change: Expanding the Concept and Addressing Uncertainties. Washington, DC: The National Academies Press; 2005.
7. Sena ET, Artaxo P. A novel methodology for large-scale daily assessment of the direct radiative forcing of smoke aerosols. *Atmos Chem Phys.* 2015;15(10):5471–5483.
8. Sundström AM, Arola A, Kolmonen P, Xue Y, de Leeuw G, Kulmala M. On the use of a satellite remote-sensing-based approach for determining aerosol direct radiative effect over land: a case study over China. *Atmos Chem Phys.* 2015;15(1):505–518.
9. Patadia F, Gupta P, Christopher SA, Reid JS. A multisensor satellite-based assessment of biomass burning aerosol radiative impact over Amazonia. *J Geophys Res Atmos.* 2008;113:D12214.
10. Sena ET, Artaxo P, Correia AL. Spatial variability of the direct radiative forcing of biomass burning aerosols and the effects of land use change in Amazonia. *Atmos Chem Phys.* 2013;13(3):1261–1275.
11. Hansen J, Ruedy R, Glascoe J, Sato M. GISS analysis of surface temperature change. *J Geophys Res Atmos.* 1999;104(D24):30997–31022.
12. Menne MJ, Williams CN, Vose RS. The U.S. historical climatology network monthly temperature data, Version 2. *Bull Am Meteorol Soc.* 2009;90(7):993–1007.
13. Alston EJ, Sokolik IN, Kalashnikova OV. Seasonal and interannual variability of atmospheric aerosols in the U.S. Southeast from ground and space based measurements over the past decade. *Atmos Meas Tech.* 2012;5(7):1667–1682.
14. Levy RC, Remer LA, Kleidman RG, et al. Global evaluation of the collection 5 MODIS dark-target aerosol products over land. *Atmos Chem Phys.* 2010;10(21):10399–10420.
15. Levy RC, Remer LA, Mattoo S, Vermote EF, Kaufman YJ. Second-generation operational algorithm: retrieval of aerosol properties over land from inversion of Moderate Resolution Imaging Spectroradiometer spectral reflectance. *J Geophys Res Atmos.* 2007;112:D13211.
16. Kahn RA, Gaitley BJ, Garay MJ, et al. Multiangle Imaging Spectroradiometer global aerosol product assessment by comparison with the Aerosol Robotic Network. *J Geophys Res Atmos.* 2010;115:D23209.
17. Kahn RA, Nelson DL, Garay MJ, et al. MISR Aerosol product attributes and statistical comparisons with MODIS. *IEEE Trans Geosci Remote Sens.* 2009;47(12):4095–4114.
18. Platnick S, King MD, Ackerman SA, et al. The MODIS cloud products: algorithms and examples from Terra. *IEEE Trans Geosci Remote Sens.* 2003;41(2):459–473.
19. Ju J, Roy DP, Shuai Y, Schaaf C. Development of an approach for generation of temporally complete daily nadir MODIS reflectance time series. *Remote Sens Environ.* 2010;114(1):1–20.
20. Schaaf CB, Gao F, Strahler AH, et al. First operational BRDF, albedo nadir reflectance products from MODIS. *Remote Sens Environ.* 2002;83(1–2):135–148.
21. Liang S, Fang H, Chen M, et al. Validating MODIS land surface reflectance and albedo products: methods and preliminary results. *Remote Sens Environ.* 2002;83(1–2):149–162.
22. Christopher SA, Gupta P, Nair U, et al. Satellite remote sensing and mesoscale modeling of the 2007 Georgia/Florida fires. *IEEE J Sel Topics Appl Earth Observ Remote Sens.* 2009;2(3):163–175.
23. Barnes CA, Roy DP. Radiative forcing over the conterminous United States due to contemporary land cover land use change and sensitivity to snow and interannual albedo variability. *J Geophys Res Biogeosci.* 2010;115(G4):G04033.





24. Levy RC, Mattoo S, Munchak LA, et al. The collection 6 MODIS aerosol products over land and ocean. *Atmos Meas Tech*. 2013;6(11):2989–3034.
25. Pozzer A, de Meij A, Yoon J, Tost H, Georgoulias AK, Astitha M. AOD trends during 2001–2010 from observations and model simulations. *Atmos Chem Phys*. 2015;15(10):5521–5535.
26. Yoon J, Burrows JP, Vountas M, et al. Changes in atmospheric aerosol loading retrieved from space-based measurements during the past decade. *Atmos Chem Phys*. 2014;14(13):6881–6902.
27. Tebaldi C, Friedlingstein P. Delayed detection of climate mitigation benefits due to climate inertia and variability. *Proc Natl Acad Sci U S A*. 2013;110(43):17229–17234.
28. Carlton AG, Pinder RW, Bhave PV, Pouliot GA. To what extent can biogenic SOA be controlled? *Environ Sci Technol*. 2010;44(9):3376–3380.
29. Portmann RW, Solomon S, Hegerl GC. Spatial and seasonal patterns in climate change, temperatures, and precipitation across the United States. *Proc Natl Acad Sci U S A*. 2009;106(18):7324–7329.
30. Hansen J, Sato M, Ruedy R. Perception of climate change. *Proc Natl Acad Sci U S A*. 2012;109(37):E2415–E2423.
31. Menon S, Akbari H, Mahanama S, Sednev I, Levinson R. Radiative forcing and temperature response to changes in urban albedos and associated CO<sub>2</sub> offsets. *Environ Res Lett*. 2010;5(1):014005.
32. Benas N, Hatzianastassiou N, Matsoukas C, Fotiadi A, Mihalopoulos N, Vardavas I. Aerosol shortwave direct radiative effect and forcing based on MODIS level 2 data in the Eastern Mediterranean (Crete). *Atmos Chem Phys*. 2011;11(24):12647–12662.